Nanoscale

Tuning the dielectric properties of metallic-nanoparticle/elastomer composites by strain

Patrick Gaiser, Jonas Binz, Bruno Gompf,* Audrey Berrier and Martin Dressel

Tunable metal/dielectric composites are promising candidates for a large number of potential applications in electronics, sensor technologies and optical devices. Here we systematically investigate the dielectric properties of Ag-nanoparticles embedded in the highly flexible elastomer poly-dimethylsiloxane (PDMS). As tuning parameter we use uniaxial and biaxial strain applied to the composite. We demonstrate that both static variations of the filling factor and applied strain lead to the same behavior, *i.e.*, the filling factor of the composite can be tuned by application of strain. In this way the effective static permittivity ε_{eff} of the composite can be varied over a very large range. Once the Poisson's ratio of the composite is known, the strain dependent dielectric constant can be accurately described by effective medium theory without any additional free fit parameter up to metal filling factors close to the percolation threshold. It is demonstrated that, starting above the percolation threshold in the metallic phase, applying strain provides the possibility to cross the percolation threshold into the insulating region. The change of regime from conductive phase down to insulating follows the description given by percolation theory and can be actively controlled.

1 Introduction

Flexible metal-dielectric composites with a high dielectric constant enable a large number of applications in charge-storage capacitors, electrostriction artificial muscles or in general in flexible organic electronics.[1–5] Several studies have investigated the mechanical tunability of the optical properties and plasmonic behavior of thin metallic films[6] or nanoparticles either in two-dimensional[7–9] or three-dimensional[10,11] metallo-dielectric composites using elastomeric substrates.

The physics behind these applications is the well-known dependence of the electric and dielectric properties of metal-dielectric composites on the metal filling factor, as described by percolation theory. The geometrical framework of this theory and the associated concepts of critical phenomena, scaling behavior and fractality are applicable on a wide variety of systems. The results are especially independent on the specific size or shape of the system under investigation. For electrical or optical measurements this size-independence is given as long as the long wavelength limit is fulfilled, which for low-frequency investigations is clearly the case. In systems consisting of randomly distributed metal nanoparticles in a dielectric host, the dc-conductivity exhibits an abrupt change when the metal concentration reaches a critical value f_c – the percolation threshold – and becomes metallic. This jump

becomes manifest in a divergence of the real part of the static dielectric constant at the insulator-to-metal transition. For a finite conductivity of the host material, theory predicts that this divergence is limited to a maximum.[12] As shown in ref. 12, the divergence can be qualitatively interpreted by the increased capacitive coupling between adjacent particles with increasing filling factor. Each pair of nearest particles forms a capacitor, which effective surface tends to infinity and its distance to zero at the percolation threshold. Therefore the effective capacity of the system diverges.

Near f_c the electrical and optical behavior is governed by scaling laws.[13] At the percolation threshold values of the real part of the permittivity of up to 10^5 have been reported in ferroelectric/metal composites.[14] At low frequencies and for a vanishing conductivity of the insulating host, the divergence of the real part of the permittivity of the composite material ε_{eff} can be described by:

$$\varepsilon_{\text{eff}}(f) \sim \frac{\varepsilon_{\text{h}}}{(f_{\text{c}} - f)^p} \quad \text{for } f < f_{\text{c}} \tag{1}$$

and

$$\varepsilon_{\text{eff}}(f) \sim \frac{\varepsilon_{\text{h}}}{(f - f_{\text{c}})^p} + \varepsilon_{\text{m}}(f - f_{\text{c}})^t \quad \text{for } f > f_{\text{c}} \tag{2}$$

where p and t are scaling factors, and ε_{h} is the permittivity of the host material and ε_{m} that of the metallic inclusions. The filling factor is given by $f = V_{\text{metal}}/V_{\text{total}}$. Experimentally f was calculated from the weighted masses and known densities of

Physikalisches Institut, Universität Stuttgart, Pfaffenwaldring 57, 70550 Stuttgart, Germany. E-mail: b.gompf@physik.uni-stuttgart.de

the constituents. For a finite conductivity σ_h of the host and a conductivity σ_m of the metal the frequency independent maximum of the real part of the permittivity of the composite at the percolation threshold is given by:

$$\varepsilon_{\text{eff}}(f_c) = \varepsilon_h \left(\frac{\sigma_m}{\sigma_h} \right)^{1-\mu} \tag{3}$$

where μ is a scaling factor.[12]

Following this route in recent years a number of papers were published on the electrical and mechanical properties of composites composed of an elastomer such as poly-dimethyl-siloxane (PDMS) together with metallic nanoparticles (NP) or carbon nanotubes.[15–18]

It was shown that the unique elastic properties of PDMS are indeed preserved even in the metallic state, *i.e.*, for metal filling factors above the percolation threshold.[19] This allows for tuning the electrical resistance of the composites by stretching the elastomer.[20] Here we systematically show that both below and even across the percolation threshold the dielectric properties can be tuned by stretching the PDMS/silver-nanoparticle composites over a wide range and that the change of the strain dependent filling factor directly follows from the elastic properties of the elastomer. Additionally it is shown that, in the case of biaxial stretching, the larger volume change leads to a stronger strain dependence of the dielectric properties compared to the uniaxial case.

2 Experimental

Ag-nanoparticle powder was bought from Ionic Liquids. They were fabricated by plasma vapor deposition and handled under Ar atmosphere. The particles are not covered by any ligand or stabilization layer. The size distribution was verified by transmission electron microscopy and the average particle size is about 35 nm with a broad distribution spanning up to 100 nm. The samples were prepared by mixing the Ag-nano-particles with PDMS (Sylgard 184, Dow Corning) in the respective volume fractions. Even though the volume fractions can be obtained from the weighted masses very accurately, the effective filling factor depends sensitively on the homogeneity of the sample. In the following the experimental filling factor calculated from the weighted masses will be called nominal filling factor. It can be determined with an accuracy of about 0.2%. Within the sample the local filling factor can exhibit larger variations due to possible inhomogeneities. In order to ensure homogeneity of all the samples, the Ag-nanoparticle powder (Ag-NP) was thoroughly ground with a mortar and mixed with pure PDMS which was prepared in a 10 : 1 ratio of elastomer and hardener. Upon mixing, the composites with filling factors near to the percolation threshold became a viscous and homogeneous liquid, an important precondition for reliable stretching experiments. Afterwards, the liquid was stirred in an ultrasonic bath and then degassed in a desiccator, for 15 min. To ensure the reproducible curing of the samples, the liquid was cast into a petri dish with a thickness not exceed-

ing 1 mm and degassed again for 10 min. Then, the liquid was cured for 120 min at 120 °C and subsequently cut into smaller pieces. Prior to the measurements the homogeneity of the samples were checked by optical microscopy. Good samples look uniformly grey and no homogeneities could be resolved. In particular, even after stretching, no buckling was to be seen.

The stretching dependent dielectric constant was determined in specifically designed set-ups, for uniaxial and biaxial stretching respectively, which allow accurate capacitance measurements under defined stretching conditions by independently determining the thickness of the sample (see Fig. 4). The capacitance itself was measured by a capacitance bridge (Andeen Hagerling, AH2550A) at 1 kHz. To account for stray fields in the finite capacitor plates and for parasitic capacitance coming from cables and the set-up all values were corrected by comparison with samples having a well-known dielectric constant (air or PDMS) by the means of an effective capacitor plate area and an offset capacitance.

3 Elastic properties of Ag-NP/PDMS composites

Before one can calculate the strain dependent filling factor of Ag-NP in the composites, the volume change of the samples under applied strain has to be known. The Poisson's ratio ν of the samples was determined from the measured thickness and length changes under uniaxial strain as measured from calibrated optical microscope pictures:

$$\nu = \frac{\dfrac{d - d_0}{d_0}}{s} \tag{4}$$

where d_0 and d are the thickness of the sample before and after stretching and $s = \dfrac{L - L_0}{L_0}$ is the applied strain. Here L_0 and L are the length of the sample before and after stretching, respectively. The Poisson's ratio is a measure of the transverse contraction of the material with respect to its longitudinal elongation. A Poisson's ratio of 0.5 would indicate that there is no volume change of the sample under strain. The PDMS
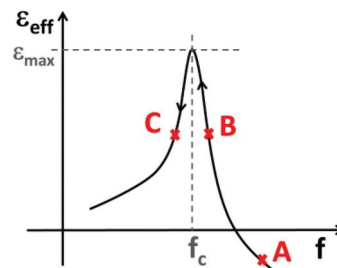
Fig. 1 Schematic illustration of the static dielectric constant ε_{eff} *vs.* filling factor *f*. At point A the dependence can be described by eqn (2) and at point C by eqn (1). The maximum is given by eqn (3). The arrows indicate the decrease of the filling factor by stretching (based on ref. 12).
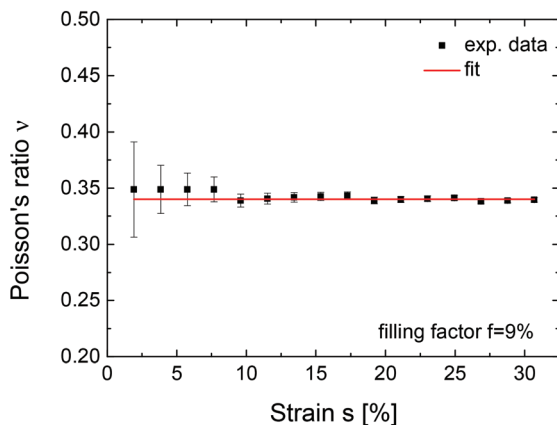
Fig. 2 The Poisson's ratio of Ag-NP/PDMS composites is independent of the applied strain and independent of the Ag-NP filling factor f in the range 0–15%.
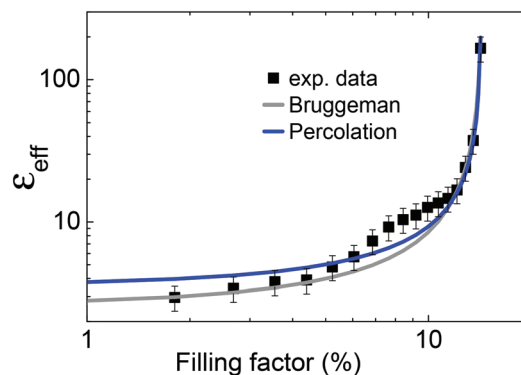

Fig. 3 Dielectric constant $\varepsilon_{\mathrm{eff}}$ as a function of the filling factor f for 19 different Ag-NP/PDMS samples. The data can be fitted by the BEMA (eqn (5)) as well as by the scaling law given in eqn (1). Error bars in the nominal filling factor are smaller than the symbol size.

samples investigated in this work have all a Poisson's ratio smaller than 0.5, indicating an increase of volume upon stretching. As an example, Fig. 2 shows the dependence of the Poisson's ratio ν on applied uniaxial strain for a sample with an Ag-NP filling factor of $f = 9\%$ measured in the range 0% to 30% stretching. For all samples under investigation the Poisson's ratio ν is basically constant, *i.e.*, independent of the applied strain and filling factor in the strain range used in our study. The fit yields $\nu = 0.34$, a value also found in our experiments for pure PDMS and all other composites under investigation up to filling factors of $f \sim 15\%$. As a consistency check, using this Poisson's ratio, the capacitance measurements yield a strain independent dielectric constant for pure PDMS of about $\varepsilon_{\mathrm{r}} = 2.7$ at 1 kHz, in good agreement with literature values.[21]

4 Dielectric properties of the composite

First we investigate the dependence of the dielectric constant $\varepsilon_{\mathrm{eff}}$ on the filling factor f of the Ag-NP. In Fig. 3 the dependence of $\varepsilon_{\mathrm{eff}}$ is plotted for 19 different samples with nominal filling factors varied between 0 (pure PDMS) and $f = 14.2\%$, a filling factor just before the samples become metallic. As expected from percolation theory, the measured dielectric constant $\varepsilon_{\mathrm{eff}}$ increases with increasing filling factor f and tends to diverge near the critical filling factor reaching values above 160. Below the percolation threshold, the experimental data can be fitted by eqn (1) resulting in a critical filling factor of $f_{\mathrm{c}} = 14.3\%$ and a critical exponent of $p = 0.8$, values in good agreement with percolation theory.[13] Due to the extremely sharp dependence of eqn (1) on f_{c} around the percolation threshold, f_{c} can be determined from the fit in Fig. 3 with an accuracy of ±0.05%. The behavior can also be described quite well by Bruggeman's effective medium approximation (BEMA):[17]

$$f \frac{\varepsilon_{\mathrm{m}} - \varepsilon_{\mathrm{eff}}}{\varepsilon_{\mathrm{eff}} + D(\varepsilon_{\mathrm{m}} - \varepsilon_{\mathrm{eff}})} = (f-1)\frac{\varepsilon_{\mathrm{h}} - \varepsilon_{\mathrm{eff}}}{\varepsilon_{\mathrm{eff}} + D(\varepsilon_{\mathrm{h}} - \varepsilon_{\mathrm{eff}})}, \quad (5)$$

where ε_{m} is the dielectric constant of the metal inclusion (Ag-NP), ε_{h} that of the host (PDMS) and $\varepsilon_{\mathrm{eff}}$ the effective dielectric constant of the composite. The depolarization factor D is a parameter describing the shape of the particles. For spheres this factor should be $D = 1/3$, for elongated ellipsoids it is expected to be between $0 < D < 1/3$, and for disc-like particles between $1/3 < D < 1$. Here one has to stress the fact that strictly speaking the BEMA is not valid anymore close to the percolation threshold, where large field fluctuations, so called hot spots, appear and therefore the assumption of a homogenous background field fails.[23] Whereas in percolation theory the critical filling factor depends neither on the size nor the shape of the particles, in the BEMA theory f_{c} is equal to the depolarization factor D and therefore strongly connected to the particle shape.[22] As a consequence for spherical particles BEMA predicts a critical filling of $f_{\mathrm{c}} = D = 1/3$, which is in contradiction to percolation theory where one expect that f_{c} equals the Scher–Zallen critical density of 15% for spherical particles.[24] In our experiments we have found critical densities close to 15%, in agreement with percolation theory. In BEMA the depolarization factor D describes the influence of the particle shape on the homogeneous background field, but close to the percolation threshold this field is governed by large field fluctuations due to increasing clustering of the particles as mentioned earlier. Therefore the shape of the individual particle becomes less and less important with increasing filling factor. D loses its original physical meaning as depolarization factor but it is still describing the critical filling factor. Interpreting D as critical filling factor and using the known dielectric constants of Ag and PDMS, eqn (5) can be used to calculate the effective $\varepsilon_{\mathrm{eff}}$ of the composite. Fitting eqn (5) to the experimental data yields a critical filling factor of $f_{\mathrm{c}} = 14.4\%$, which indicates the same value for f_{c} as that found earlier from eqn (1). Again, this value is very close to the Scher-Zallen critical density. As mentioned above, the filling factors for all 19 samples shown in Fig. 3 were determined from the weighted masses and the bulk densities of the individual constituents. The relative small discrepancy between the calculated and

measured ε_{eff} in Fig. 3 gives an estimate for the good reproducibility of our results. From eqn (3) it can be seen that our samples with the highest filling factor are very close to the percolation threshold. Assuming reasonable values for the conductivity of PDMS of about $\sigma_0 \sim 10^{-8}$ Ω cm^{-1} and the Ag-NP conductivity of about $\sigma_m \sim 10^6$ Ω cm^{-1}, one obtains an estimate for the maximum dielectric constant of about 630, which is of the same order of magnitude as the measured value of 160 for the sample with nominal $f = 14.2\%$ below the percolation threshold. For this estimation we use a critical exponent $\mu = 0.8$, the value predicted by percolation theory and also found in recent measurements in carbon nanotube composites.[25]

5 Uniaxial and biaxial strain

The effect of uniaxial strain s on a PDMS sample leads, on the one hand, to an elongation of the sample in the direction of the applied force (ΔL) and on the other hand to sample shrinkage in the other two directions (see Fig. 4). Under the assumption of an isotropic stretching behavior and neglecting higher order terms this leads to a volume change which can be described by

$$\frac{\Delta V}{V} = s(1 - 2\nu) \text{ uniaxial.} \tag{6}$$

In the case of biaxial stretching the sample is isotropically stretched in the film plane while only the thickness shrinks. This leads to twice the volume change as in the uniaxial case

$$\frac{\Delta V}{V} = 2s(1 - 2\nu) \text{ biaxial.} \tag{7}$$

Assuming that only the volume of the elastomer is increased upon stretching by $V_g = V + \Delta V$ and the volume of the embedded Ag-NP stays constant the strain dependent filling factors are given by

$$f(s) = \frac{V(\text{Ag NP})}{V_g} = \frac{f_0}{1 + 2s(1 - 2\nu)} \text{ uniaxial} \tag{8}$$

and

$$f(s) = \frac{V(\text{Ag NP})}{V_g} = \frac{f_0}{1 + 2s(1 - 2\nu)} \text{ biaxial} \tag{9}$$

where f_0 is the filling factor for the unstretched sample. From these formulas one directly sees that if the volume stays constant ($\nu = 0.5$) upon stretching, the filling factor is also constant and there would be no change of the dielectric constant by applying strain as it is the case for PDMS.

Fig. 4 displays a schematic drawing of both set-ups used in this work. The change in the dielectric constant induced by the applied strain is measured by small capacitor plates placed below and above the samples, in the middle of the stretched region. The two plates are pressed against the sample by small springs to compensate for the strain induced shrinking of the sample height. All strain dependent measurements were performed with unstretched freshly prepared samples. All the results presented in this manuscript have been successfully reproduced by independently produced samples. All the samples gave rise to identical behavior when stretched the first time. Some of the samples have been stretched up to 60%, which is over the threshold to the plastic regime of the sample, they have shown an hysteresis of about 20% upon release of the strain. However after the complete stretch/release cycle was completed the capacitance value ended up at the same point, within the error bars. For samples stretched within the elastic regime, even smaller deviations are to be expected. However, since in loading–unloading cycles the samples exhibit a slight hysteresis, we present only first time stretched data here.

Fig. 5 shows the strain dependent dielectric constant ε_{eff} for an Ag-NP/PDMS composite with a nominal starting filling factor of $f_0 = 10.6\%$ up to a strain of 54% in the case of uniaxial stretching. The strain induced reduction of the filling factor f leads to a continuous decrease of the effective dielectric constant of the composite. At the highest applied strain the filling factor is reduced to $f = 9.2\%$, i.e., roughly by 10%.

Over the same range the effective dielectric constant is reduced from 11.8 to 8.3 corresponding to a reduction of roughly 30%. By inserting eqn (8) into eqn (5) the expected
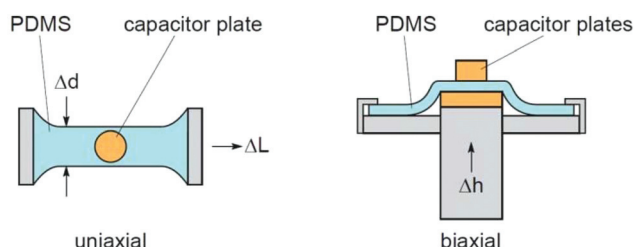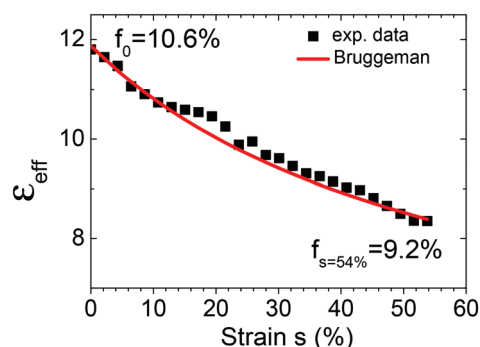

Fig. 4 Scheme of both stretching set-ups. (a) Uniaxial strain ΔL leads to a shrinking of the sample in the two other directions; (b) biaxial case: the strain applied by Δh stretches the sample isotropically; only the thickness shrinks. The thereby induced changes in the dielectric constant are measured by small capacitor plates as illustrated.

Fig. 5 Uniaxial-strain dependent dielectric constant of an Ag-NP/PDMS composite with a nominal starting filling factor of $f_0 = 10.6\%$. The line curve is calculated by inserting eqn (8) into eqn (5) without using any free fit parameters.
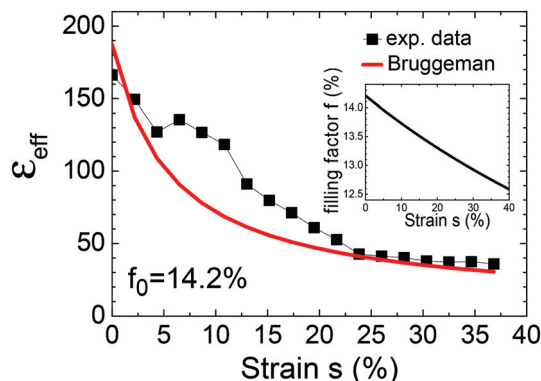
Fig. 6 Dielectric constant *vs.* uniaxial strain of an Ag-NP/PDMS composite with a nominal starting filling factor of $f_0 = 14.2\%$ close to the percolation threshold. The inset helps converting the strain dependent filling factor based on eqn (8). The line curve is calculated by inserting eqn (8) into eqn (5).

change of the effective dielectric constant can be calculated without using any free fit parameters. The agreement between the experimental data and the calculated values is extremely good. This has two main implications: the BEMA nicely describes the effective dielectric constant of the composite if $D = f_c$ is interpreted as the critical filling factor and the strain dependent change of the filling factor can be simply described by the Poisson's ratio ν of the composite.

In Fig. 6, the result for an Ag-NP/PDMS composite with a nominal starting filling factor of $f_0 = 14.2\%$ is shown. At this high starting filling factor close to the critical value f_c, an applied uniaxial strain of 36% reduces the dielectric constant by nearly a factor of 5, whereas the filling factor is only reduced from 14.2% to about 12.6%. The inset shows the strain dependent filling factor calculated from eqn (8). The line curve in the main panel gives the calculated effective dielectric constant obtained by inserting eqn (8) into eqn (5). For filling factors close to the percolation threshold the strain

dependent capacitance measurements exhibit much larger fluctuations, leading to larger discrepancies between measurement and calculation. The main reason for the fluctuations is the presence of losses in the sample due to a non-vanishing conductivity, *i.e.*, ε cannot be treated as purely real anymore.

These fluctuations become even larger for filling factors above the percolation threshold. In fact for uniaxial stretching it was not possible to cross the percolation threshold by starting with a metallic sample due to the required too high strain. From eqn (9) one expects a larger change of the filling factor for the same strain in the case of biaxial stretching. Therefore we perform additional measurements under biaxial strain for different nominal starting filling factors f_0 ranging from 5% to 11%. In Fig. 7 the results are shown for three different f_0. In the figure the changes of ε_{eff} due to the applied biaxial strain s are directly plotted as a function of the filling factor $f(s)$ as calculated by eqn (9). For all three samples the strain was varied from 0 to about 40%. The additionally continuous line is calculated from the BEMA (eqn (5)) without any free fit parameter. The very good agreement between calculation and measurement shows that the filling factor can also be nicely tuned by applying biaxial strain.

In contrast to the case of uniaxial stretching, it is possible now to cross the percolation threshold under biaxial stretching. In Fig. 8 the change of the dielectric constant under biaxial strain is shown for an Ag-NP/PDMS composite with a starting filling factor slightly above the percolation threshold ($f_c \sim 15\%$). For clarity on the x-axis $f - f_c$ is plotted to demonstrate that the huge changes due to the divergence at f_c happens within ±1% left and right of the percolation threshold. It is to be noted that first order phase transitions are governed by large fluctuations at the critical point. For metal-to-insulator transitions this is manifested in huge conductivity fluctuations around the percolation threshold which in principle leads to fluctuating values. Every individual measured sample will therefore follow only qualitatively the predicted overall behaviour at the critical density. Above the
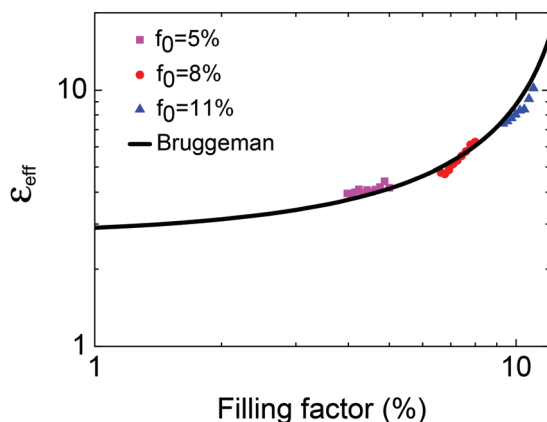
Fig. 7 Dielectric constant *vs.* filling factor f under biaxial stain for three different starting filling factors f_0. The respective filling factor changes were calculated by eqn (9) and the ranges correspond to maximum applied strains of about 40%. The continuous line is calculated from eqn (5) without using any free fit parameters.
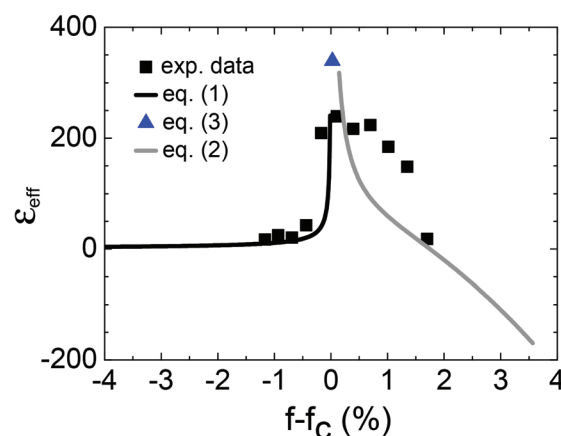
Fig. 8 Dielectric constant *vs.* biaxial strain for an Ag-NP/PDMS composite with a starting filling factor above the percolation threshold. The lines and the triangle are calculated from eqn (1)–(3), respectively.

percolation threshold, ε_{eff} is not purely real anymore and the fluctuations are large due to the fragile conducting networks in this region. Nevertheless biaxial stretching leads in this case first to an increase of ε_{eff}, reaching values of about 250 and then under further stretching to a steep decrease, following the sketched behavior of Fig. 1, going from point A to C. The lines and the triangle are calculated from the eqn (1)–(3), respectively, according to the scheme in Fig. 1. Although the agreement with theory above the percolation threshold is not as perfect as below the percolation threshold, the overall behavior is quantitatively well reproduced. For instance the zero-crossing of ε_{eff} occurs slightly above f_c. Between f_c and the zero-crossing of ε_{eff}, the composite has a positive ε_{eff} although some narrow conducting paths exist (point B in Fig. 1), a behavior already shown for thin percolating metal films.[26]

6 Conclusions

In this investigation we have shown that it is possible to tune the dielectric constant of Ag-NP/elastomer composites by applying uniaxial and biaxial strain over a wide range. The strain dependent dielectric function follows thereby the strain dependent filling factor. The strain dependent filling factor is given by the expected volume change upon strain and depends only on the Poisson's ratio of the composite. Owing to the larger volume change in the case of biaxial strain, the tuning capability is larger compared to the uniaxial case. Below the percolation threshold the dielectric behavior can be nicely described by percolation theory as well as by the BEMA. Percolation theory is even able to correctly describe the divergence of ε_{eff} across the percolation. Here huge values of the dielectric constant of over 250 can be observed. This tunability opens up many novel applications in sensing or plastic electronics, where a controlled tuning of the dielectric/conductive properties of the composite materials is required.

Acknowledgements

Notes and references

1 J. A. Rogers, T. Someya and Y. Huang, *Science*, 2010, **327**, 1603.

2 T. Sekitani, H. Nakajima, H. Maeda, T. Fukushima, T. Aida, K. Hata and T. Someya, *Nat. Mater.*, 2009, **8**, 494.

3 Q. M. Zhang, H. Li, M. Poh, F. Xia, Z.-Y. Cheng, H. Xu and C. Huang, *Nature*, 2002, **419**, 284.

4 T. Mirfakhrai, J. D. W. Madden and R. Baughman, *Mater. Today*, 2007, **10**, 30.

5 T. Sekitani, U. Zschieschang, H. Klauk and T. Someya, *Nat. Mater.*, 2010, **9**, 1015.

6 S. Rehwald, M. Berndt, F. Katzenberg, S. Schwieger, E. Runge, K. Schierbaum and D. Zerulla, *Phys. Rev. B: Condens. Matter*, 2007, **76**, 085420.

7 X. Zhu, L. Shi, X. Liu, J. Zi and Z. Wang, *Nano Res.*, 2010, **3**, 807.

8 M. G. Millyard, F. M. Huang, R. White, E. Sprigone, J. Kivioja and J. Baumberg, *Appl. Phys. Lett.*, 2012, **100**, 073101.

9 T. Vossmeyer, C. Stolte, M. Ijeh, A. Kornowski and H. Weller, *Adv. Funct. Mater.*, 2008, **18**, 1611.

10 Y. Kim, J. Zhu, B. Yeom, M. Di Prima, X. Su, J.-G. Kim, S. J. Yoo, C. Uher and N. A. Kotov, *Nature*, 2013, **500**, 59.

11 D. Ryu, K. J. Loh, R. Ireland, M. Karimzada, F. Yaghmaie and A. M. Gusman, *Smart Struct. Syst.*, 2011, **8**, 471.

12 A. L. Efros and B. I. Shklovskii, *Phys. Status Solidi*, 1976, **76**, 475.

13 J. P. Clerc, G. Giraud, J. M. Laugier and J. M. Luck, *Adv. Phys.*, 1990, **39**, 191.

14 C. Pecharroman, F. Esteban-Betegon, J. F. Bartolome, S. Lopez-Esteban and J. S. Moya, *Adv. Mater.*, 2001, **13**, 1541.

15 P. Du, X. Lin and X. Zhang, *J. Phys. D: Appl. Phys.*, 2013, **46**, 195303.

16 M. Park, *et al.*, *Nat. Nanotechnol.*, 2012, **7**, 803.

17 D. A. G. Bruggeman, *Ann. Phys.*, 1935, **24**, 636.

18 K.-Y. Chun, Y. Oh, J. Rho, J.-H. Ahn, Y.-J. Kim, H. R. Choi and S. Baik, *Nat. Nanotechnol.*, 2010, **5**, 853.

19 A. T. Sepulveda, *et al.*, *Nanoscale*, 2013, **5**, 4847.

20 M. Park, H. Kim and J. P. Youngblood, *Nanotechnology*, 2008, **19**, 055705.

21 Dow Corning, Sylgard 184 product information.

22 T. C. Choy, *Effective Medium Theory*, Oxford Science Publications, 1999.

23 V. M. Shalaev and A. K. Sarychev, *Phys. Rev B: Condens. Matter*, 1998, **57**, 13265.

24 H. Scher and R. Zallen, *J. Chem. Phys.*, 1970, **53**, 3759.

25 L. Wang and Z.-M. Dang, *Appl. Phys. Lett.*, 2005, **87**, 042903.

26 M. Hövel, B. Gompf and M. Dressel, *Phys. Rev. B: Condens. Matter*, 2010, **81**, 035402.